17th Brazilian Congress of Thermal Sciences and Engineering
November 25th-28th, 2018, Águas de Lindóia, SP, Brazil

ENCIT-2018-0833
THE USE OF INFRARED IMAGE FOR THE DETECTION OF THE THYROID

Henrique Massard da Fonseca
Helcio Rangel Barreto Orlande
Department of Mechanical Engineering – COPPE/UFRJ, CP 68503, CT, Federal University of Rio de Janeiro, Rio de Janeiro-RJ, 21941-972, Brazil
hmassardf@gmail.com
helcio@mecanica.coppe.ufrj.br

Marcos Santos
Cellular Morphogenesis Laboratory, Institute of Biomedical Sciences, Federal University of Rio de Janeiro, Rio de Janeiro-RJ, 21949-900, Brazil
santosmfh@gmail.com

Elmo Fabiano Monteiro Pereira Jr.
Copa Star Hospital - Rua Figueiredo de Magalhães, 700, Copacabana, Rio de Janeiro-RJ, 22031-012, Brazil
Paulo Niemeyer Brain Institute - Rua do Rezende, 156, Centro, Rio de Janeiro - RJ, 20231-092, Brazil
Rio Ensino Médico Ltda - Rua Lauro Muller, 56, Apt 1110, Botafogo, Rio de Janeiro – RJ, 22290-160, Brazil
elmo.pereira@winfocus.org

Abstract. *The early detection of cancer when the tumor is relatively small is crucial for the success of treatment protocols. Today, the most widely used techniques for the image detection are magnetic resonance (MRI), computerized tomography (CT) scan, and x-ray (mammography). Temperature measurements taken with an infrared camera can also be used for tumor detection. This paper presents preliminary results towards the development of a method of using infrared temperature measurements for tumor detection in the thyroid. A protocol available in the literature was also modified in this work, in order to enhance the thermal contrast between the thyroid and the surrounding tissues and organs.*

Keywords *Thyroid tumor, Non-Intrusive Technique, Bioengineering, Infrared Camera, Diagnostic Imaging Technique.*

1. INTRODUCTION

Infrared thermography application in medicine is based on temperature measurements related to the infrared radiation emitted by the tissue being studied or by the skin. The temperature distribution depends on the metabolic activity, the blood perfusion and ambient conditions (Santa Cruz, *et al*., 2009). Anomalies in internal organs can result in variations in temperature distribution on the skin due to the increase of metabolic activity. The vascularity of the tumor, for example, plays a crucial role in its growth rate and metastasis (Gavriolaia, *et al.*, 2009). Thus, the temperature distribution measured on the skin surface can be used for the indication of diseases, like cancer for example. Infrared temperature measurements have the advantages of being non-invasive, non-destructive and with a relative low cost. This technique is quite powerful in the sense that a temperature mapping of a specific area can be obtained in a fast and safe manner (Han, *et al*., 2013).

The massive use of infrared thermography is, however, very limited. Problems associated with the temperature sensibility in cases where the tumor is small and deep are still a challenge. To deal with this limitation, several works available in the literature models the temperature distribution on the region of interest, like the neck and the breast (Gavriloaia, *et al*., 2009; Han, *et al*., 2015; Jin, *et al*., 2014; Wahab, *et al*., 2015; Agyingi, *et al*., 2015; Carlak, *et al*., 2016; Amri, *et al*., 2016). These models consider the thermophysical properties of the several elements that make up the human body, like muscle, organs, fat and the metabolism itself. Besides that, transport phenomena like blood perfusion and the convection induced by the respiration are also considered in these models. In the above-mentioned works the determination of the temperature field was investigated from the know properties of the health and cancerous tissues. Unfortunately, the use of models for the prediction of tumors is not simple, because the properties of the tissues are not precisely known, and the geometry varies significantly from one person to another.

This work is intended to use image processing techniques instead of trying to model the temperature profile in the neck. Image processing can be used for two different purposes: improve the visual appearance of images for the human perception and prepare images for the measurement of its inherent features and structures, like edges, color, texture or some combination of these factors (Russ, 2002). Image processing techniques are used in many applications, such as in medicine for the enhancement of magnetic resonance or x-ray imaging, in aeronautics and space for the reconstruction of

noisy images sent from space, and automated visual inspection to improve the productivity and the quality of certain product.

There are several aspects that can be pursued when using some image processing technique, and the most important are the image reconstruction, image enhancement, image compression and image filtering. The particular aspect that will be explored in this work is the image enhancement, since the idea is to increase the contrast between the thyroid gland and its surrounding elements, such as muscles, veins and arteries. The aim of enhancement is to deliver a processed image more suitable (for a specific application) than the original one. There is no general theory for image enhancement. When an image is processed for visual interpretation, the viewer is the responsible for judging the performance of a particular method (Gonzales and Woods, 1992).

In this work, a histogram modification technique was used to enhance the image contrast between the thyroid gland and its neighbor organs/tissues. The visual contrast of an image can be improved by adjusting the grayscale so that the histogram of the resulting image is flat. This increase in visual contrast is an artificial enhancement due to a more judicious choice of the relative intensities, represented by the quantization levels of the original image (Hummel, 1977).

The experimental measurements were performed with volunteers from the Laboratory of Transmission and Technology of Heat from the Federal University of Rio de Janeiro (LTTC/COPPE/UFRJ), were this research is carried out. Their thyroid gland region was precisely determined by an ultrasound exam held in the Rio de Janeiro Brain Institute State Hospital. Afterwards, the ultrasound images were superposed with the infrared ones and the image processing techniques *histogram equalization* and *contrast limited adaptative histogram equalization* (CLAHE) were applied. Both *histogram equalization* and *contrast limited adaptative histogram equalization* were utilized from the built-in function *histeq* and *adapthisteq* respectively, available at the Image Processing © Toolbox from Matlab©.

2. TEMPERATURE MEASUREMENT AND IMAGE PROCESSING

A set of volunteers were chosen from the laboratory LTTC/COPPE/UFRJ. These volunteers were named P1, P2 and P3. In order to perform the temperature measurements of the desired region of the volunteers, they were positioned in dorsal decubitus position, with the infrared camera focusing on their neck, as shown by Fig. 1.

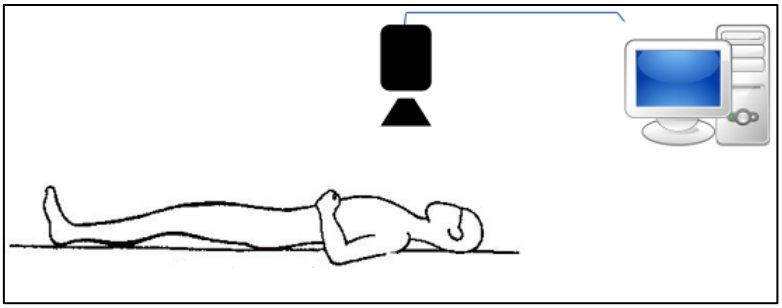

Figure 1 – Infrared temperature measurement procedure of the volunteers.

In this work, the experimental temperature measurements were performed with a A325 FLIR infrared camera. The electrical signal given by the camera is a function of the incident electromagnetic radiation over its sensor. This electrical signal is then converted to a Digital Level (DL), with linear increasing transfer functions that result from a calibration procedure. The camera has an uncooled microbolometer detector of 320 x 240 pixels and is sensitive in the range between 7.5 and 13.0 μm. The infrared camera used in this work has its sensor calibrated to perform temperature measurements at 30 cm from the target, so the camera was fixed in a tripod 30 cm above the volunteer´s neck.

The measurement campaign was performed with the volunteers by following a protocol described by (Kandlikar, *et al*., 2017). This protocol is necessary to avoid any bias caused by the ingestion of high quantities of coffee or fat, for example, prior to the experiment. Some of the protocol steps are the following (Kandlikar, *et al*., 2017):

1) Large meals, excessive consumption of beverages such as tea or coffee, as well as smoking and alcohol consumption, should be avoided prior to examination;
2) Avoid factors that may affect the thermogram, including sunbathing (up to five days prior to examination) and application of cosmetics, lotions or antiperspirants;
3) The patient should be in the examination room for at least 15 minutes prior to examination, in loose fitting cloths to get acclimatized to the environment;
4) The room temperature should be maintained between 18 ºC and 25 ºC.

It was also noted in the literature (Kandlikar, *et al*., 2017) that the cooling of the region under study increases the contrast, since the natural reheating of each organ may vary, because of the different thermophysical properties, metabolism, perfusion rate, etc. Thus, the neck of the volunteers was cooled for 3 minutes with a piece of cloth that was previously placed in the refrigerator at a temperature around 15 ºC.

Figure 2 presents a sample image of the procedure developed herein. The temperature scale is located to the right of Fig. 2, which represents the color palette associated to this image. The lighter colors are equivalent to the higher temperatures, whereas the darker colors represent the lower temperatures.

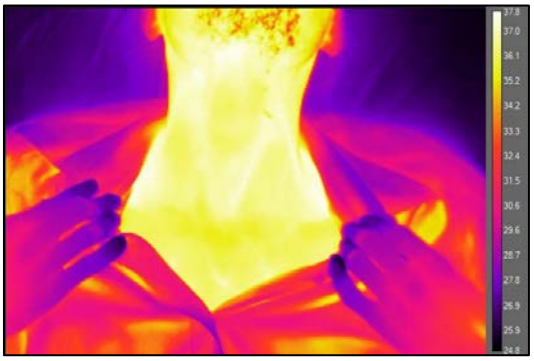

Figure 2. Thermographic image of a volunteer.

Figure 2 shows that specific differences may exist for each region of the body, which are influenced by internal organs and its characteristics in terms of heat exchange with its neighbor elements, like the trachea, with a high flow rate of cold air, and great veins, muscles and arteries from the neck. These are precisely the behavior that will be explored in this work for the detection of the thyroid. It can also be observed in Fig. 2 that a post processing technique should be performed to extract relevant information for the detection of possible pathologies. Two standard image processing techniques was used in this work to enhance the contrast of the gray level image, namely the *histogram equalization* and the *contrast limited adaptative histogram equalization* (CLAHE) (Russ, 2002; Acharya and Ray, 2005).

In an image with low contrast, many pixels occupy a small region of the available range of intensities. By properly modifying the histogram, each pixel can be reassigned with a new intensity value so that the dynamic range of gray levels is increased. The principle is to stretch the dynamic range of the pixel values in such a way that the lighter pixels may turn still lighter and the comparatively darker pixels will be darkened, providing an image with an increased contrast. The so-called *histogram equalization* is a technique where the gray scale of the input image is tuned by converting its gray level histogram onto a uniform histogram. In a statistical sense, the information provided by an image is related to the probability of occurrence of gray levels in the form of a histogram of the image. By uniformly distributing the probability of occurrence of gray levels in the image, it becomes easier to distinguish the information content of the image (Acharya and Ray, 2005).

It is important to mention that the process of image enhancement does not increase the information content of the image data. It increases the dynamic range of the chosen features (contrast for example), aiming at improving the visual detection of the image features (Acharya and Ray, 2005; Hummel, 1977). In this regard, image processing is like word processing or food processing. It is possible to rearrange things to make a product that is more pleasant or interpretable, but the total amount of data does not change. In the case of images, this generally means that the number of bytes (or pixels) is not reduced (Russ, 2002).

An example extracted from Mathworks (2018) will be presented to illustrate this method. As it can be seen from Fig. 3.a, the contrast between the photograph of the tire and the snow stains is very poor. The associated histogram (to the right of Fig. 3.a) of this image shows that there is a peak in the black region of the image, coded with the lower range of gray levels, to the left of the histogram. If we spread out all the available information provided by the gray levels, as presented in Fig. 3.b, it can be observed that now all the details of the image are presented more clearly, showing that just by properly manipulating the data it is possible to enhance the overall perception of the image.

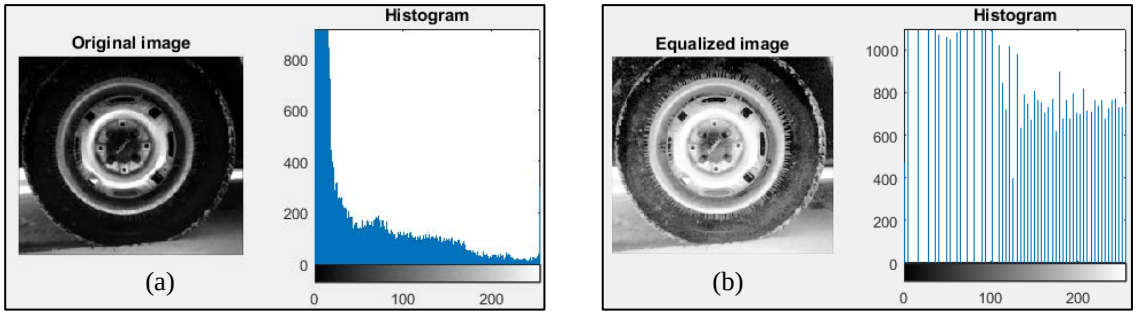

Figure 3. Example of the histogram equalization method. (a) Original image with its associated histogram and (b), the same image with its histogram converted to a normal distribution (Mathworks, 2018).

Image enhancement techniques are divided into two main categories, in terms of the spatial and frequency domains. For the first case, the manipulation is performed directly on the pixels of the image. For the frequency domain techniques, the idea is to modify the Fourier transform of an image (Gonzales and Woods, 1992). The histogram equalization technique falls into those of the spatial domain.

Spatial domain processes can be denoted by the expression (Gonzales and Woods, 1992):

$$g(x,y) = T[f(x,y)] \tag{1}$$

where $f(x,y)$ is the input image, $g(x,y)$ is the processed image, and T is an operator on f, defined over some region (x,y). The simplest form of T is when the region is of size 1x1 (that is, a single pixel). In this case, g depends only on the value of f at (x,y), and T becomes a gray-level transformation function of the form

$$s=T(r) \tag{2}$$

where, for simplicity in notation, r and s are variables denoting, respectively, the gray level of $f(x,y)$ and $g(x,y)$ at any point (x,y) (Gonzales and Woods, 1992). Larger regions allow considerably more flexibility. The general approach is to use a function of values of f in a predefined neighborhood of (x,y) to determine the value of g at (x,y). One of the principal approaches in this formulation is based on the so-called masks (or filters, kernels, templates or windows). Basically, a mask is a small (for example 3x3) 2-D array, such as the one shown by Fig. 4, in which the values of the mask coefficients determine the nature of the process, such as image sharpening. Enhancement techniques based on this type of approach are often referred to as mask processing or filtering.

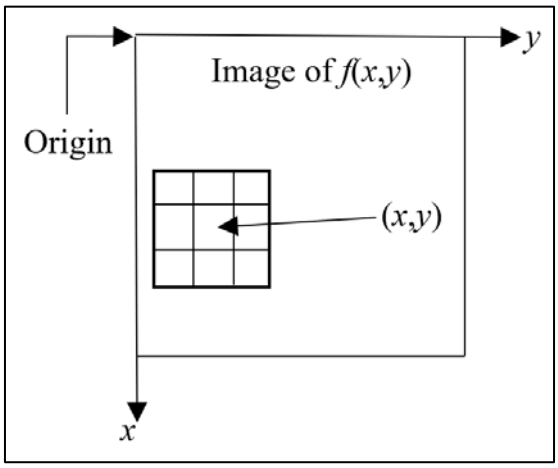

Figure 4. A 3x3 neighborhood about a point (x,y) in an image.

The histogram of a digital image with gray levels in the range $[0,L\text{-}1]$ is a discrete function $h(r_k)=n_k$, where r_k is the kth gray level and n_k is the number of pixels in the image having gray level r_k and L is the number of gray levels (256 in an 8-bit image, for example). It is common practice to normalize a histogram by dividing each of its value by the total number of pixels in the image, denoted by n. Thus, a normalized histogram given by $p(r_k)=n_k/n$, for $k=0,1,\ldots,L\text{-}1$. Hence, $p(r_k)$ gives an estimate of the probability of occurrence of gray level r_k. It is to be noted that the sum of all components of a normalized histogram is equal to 1.

The gray levels in an image may be viewed as random variables in the interval $[0,L\text{-}1]$. The probability of occurrence of gray level r_k in an image is approximated by

$$p_r(r_k) = n_k / n, \quad k = 0,1,2,\ldots,L-1 \tag{3}$$

where n is the total number of pixels in the image and n_k is the number of pixels that have the gray level r_k, and L is the total number of possible gray levels in the image. In addition, a transformation function (Eq. (2)) of particular importance in image processing has the form (Gonzales and Woods, 1992):

$$s_k = T(r_k) = \sum_{j=0}^{k} p_r(r_j), \quad k = 0,1,2,\ldots,L-1 \tag{4}$$

where $p_r(r)$ denote the probability density functions (PDF) of the random variable r. The right hand side of Eq. (4) is recognized as the discrete cumulative distribution function (CDF) of random variable r. By combining Eq. (4) (the transformation function) with Eq. (3) (the probability of occurrence of each gray level of the original image), one obtains (Gonzales and Woods, 1992):

$$s_k = T(r_k) = \sum_{j=0}^{k} p_r(r_j) = \sum_{j=0}^{k} n_j / n \,, k = 0,1,2,...,L-1 \tag{5}$$

It cannot be proved in general that this discrete transformation will produce the discrete equivalent uniform probability density function, which would be a uniform histogram. However, the use of Eq. (5) does have the general tendency of spreading the histogram of the input image (Gonzales and Woods, 1992).

Although the above method is simple, it does not take into account local details. Large peaks in the histogram can be caused by uninteresting areas, such as background noise. In this case the global histogram equalization has the undesired effect of overemphasizing noise. The technique does not adapt to local contrast requirements; minor contrast differences can be entirely missed when the number of pixels falling in a particular gray range is small (Russ, 2002; Zuiderveld, 1994). Histogram equalization can also be performed locally, where the equalization is based on the histogram of the portion of the image under a two-dimensional sliding window that is centered over the pixel in the center of the rectangular region and its gray level is modified by equalization procedures (see Fig. 4). The process of local equalization enhances the contrast near edges, revealing details in both light and dark regions (Russ, 2002; Zuiderveld, 1994).

When the histogram equalization is applied in such windows, it is called *Adaptative Histogram Equalization* (AHE). This method first appeared in the 70´s and was developed by a research group from the Hughes Aircraft Company. It was developed at that time for cockpit displays, because they suffered from poor quality (Ketcham, *et al*., 1974). Of course, in the 70´s the capabilities of onboard computers for airplanes required a cheap computational method for image enhancement. This is one of the advantages of the AHE: It is extremely fast (for the small number of bits and pixels at that time) and easy to implement and could work at TV rates. The images used were digitized from a flying spot scanner, a digital scan converter and radar direct recording. It is also interesting to mention that in this same work, Ketcham *et al*. (1976) already mentioned the use of the AHE for infrared imaging. The main issue was the restriction of dynamic range of the cathode-ray tubes. The infrared imaging had a much broader dynamic range, and information was lost because of saturation and compression of the video (Ketcham, *et al*., 1974).

Later, in 1986, Pizer *et al*. (1986) developed the *Contrast Limited Adaptative Histogram Equalization* (CLAHE). If the image has a great area of background or any other homogeneous region, even with a local approach for the histogram equalization, the noise may be overemphasized. The transformation function (Eq. (5)) might lead a limited range of input intensity values of noise (or background) to a wide range of output intensity values. But limiting the maximum of contents of the histogram bins will limit the amount of contrast enhancement, and consequently the enhancement of noise (Pizer, *et al*., 1986). After clipping the histogram, the pixels that were clipped are equally redistributed over the whole histogram to keep the total histogram count identical, as shown in Fig. 5 (Zuiderveld, 1994).

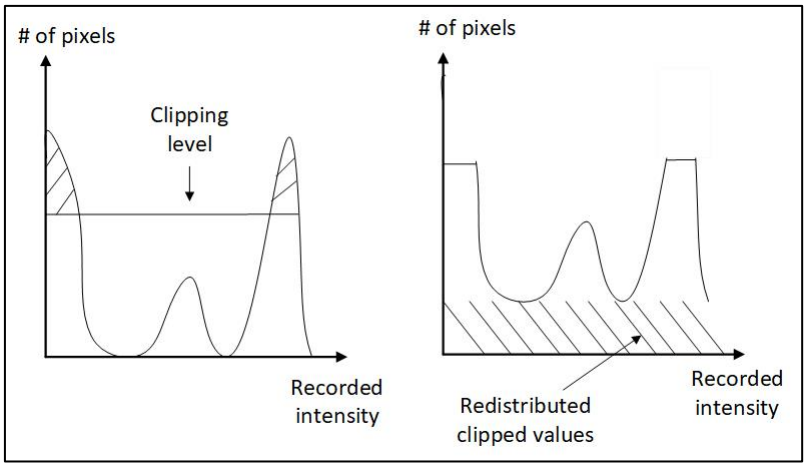

Figure 5. Histogram clipping procedure for the CLAHE implementation. Extracted from (Pizer, *et al*., 1986)

In order to precisely determine the thyroid region for each volunteer, ultrasound exams were performed by Dr. Elmo Pereira Junior, at Paulo Niemeyer Brain Institute was performed. Figure 5 shows one of the volunteers being examined by Dr. Pereira, and the portable equipment used for the ultrasound imaging, namely the SonoSite M-Turbo.

Figure 6. The ultrasound exam and the portable device used

The resulting thyroid region for volunteers P1, P2 and P3 are presented in Fig. 6.a, Fig. 6.b and Fig 6.c, respectively. From this image, it can be observed that specific characteristics makes the geometric shape of the organ to change drastically. Therefore, the ultrasound exam is a crucial validation procedure, since there is no standard shape and location for the thyroid.

Figure 7. The resulting thyroid region for the volunteers (a) P1, (b) P2 and (c) P3

(a) (b)

3. RESULTS

The images obtained with the infrared camera were processed and combined with the photos taken from the regions of the thyroid gland, obtained with the ultrasound exam. Figures 7.a-c (volunteers P1, P2 and P3 respectively) show that there is a region in the thermographic image which presents a pattern in very good agreement with the information provided by the ultrasound exam, despite the different shapes of the thyroids of the different volunteers.

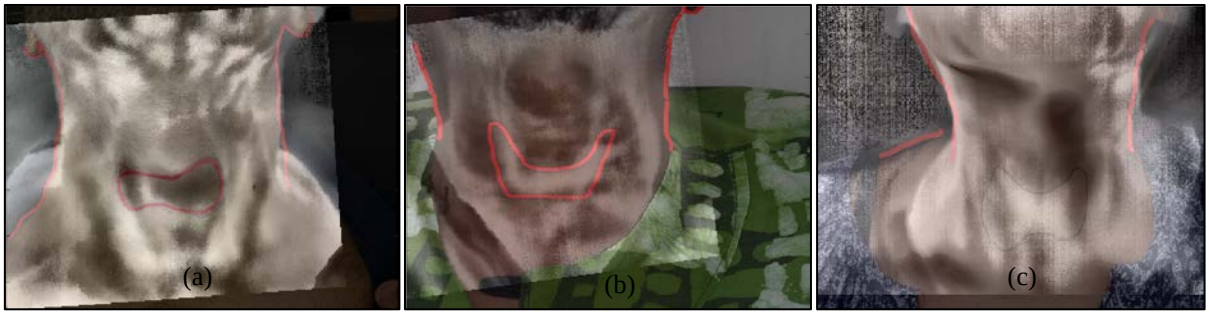

Figure 8. The resulting superimposing of the thermographic image and the photo of the thyroid region for the volunteer (a) P1, (b) P2 and (c) P3

In order to avoid non-interesting regions and focus just on the area of the thyroid gland, a trim in the infrared images was performed. Figure 8.a-c presents the regions that will be evaluated from this point on, for volunteer P1, P2 and P3. The black rectangle in each volunteer highlights the region where the infrared image will be evaluated.

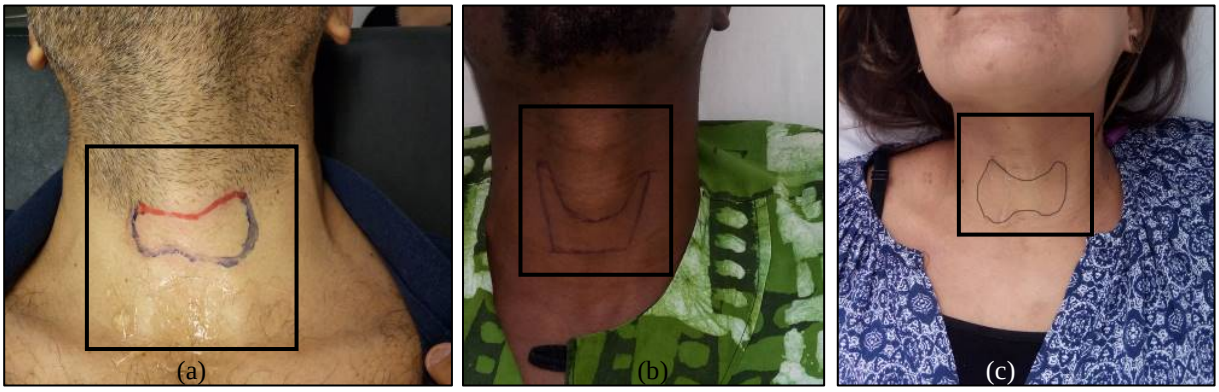

Figure 9. The regions of the image that will be evaluated for volunteers (a) P1, (b) P2 and (c) P3

For the thyroid region determination, both the histogram equalization and the contrast limited adaptative histogram equalization (CLAHE) techniques were used. Figure 10.a-c (volunteers P1, P2 and P3 respectively) presents the results obtained for the histogram equalization technique, for the region delimited in Fig. 9.a-c. It can be observed from these figures that the contrast was enhanced at the location of the thyroid gland, but since the histogram equalization takes into account the entire image information for the enhancement, details of the contrast can be lost when the number of pixels falling in a particular gray range is small. Therefore, the CLAHE will also be applied in this work as described next.

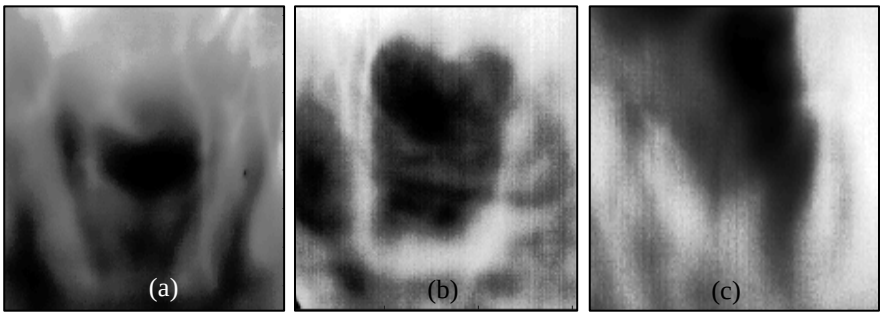

Figure 10. Histogram equalization at the thermographic images for the volunteer (a) P1, (b) P2 and (c) P3.

The CLAHE has two main parameters to be tuned prior to the application of the method: The number of windows and the clipping limit. The number of windows defines the number of tiles that the original image will be divided for the histogram equalization. A large number of windows makes them very small and the contrast will be very sensitive to point variations, in special to noise. In addition, the computation time will increase, since more data is needed to be computed. The clip limit is related to the clipping level, which restrains the weight of pixels that represents high peaks in the histogram. These are generally uniform regions representing areas of small interest, such as background or uniform areas with low signal-to-noise ratio. The number of these pixels should be clipped to allow other meaningful pixels for the interpretation of the image to be taken into account. In practice, the clipping limit restricts the contrast enhancement. A high clipping limit results in the standard AHE, i.e. no clipping. The clip limit set to 0 would uniformly distribute the image pixels across the entire histogram, which would result in the lowest possible contrast value.

Figure 11 shows the image enhancement obtained with 2x2, 2x4, 2x6, 4x2, 4x4, 4x6, 6x2x 6x4 and 6x6 tiles, respectively (*m* x *n* tiles means that the image has *m* tiles in the *x* direction and *n* tiles in the *y* direction), for the region presented in Fig. 9.c. This figure show that 4x6 and 4x4 tiles result in the best compromise between the contrast and the noise magnification of the image. The 4x6 window was then chosen for this particular image (volunteer P3). Finally, as described above it can be seen that for the 6x6 tiles, the noise is much more noticeable than the 2x2 tile.

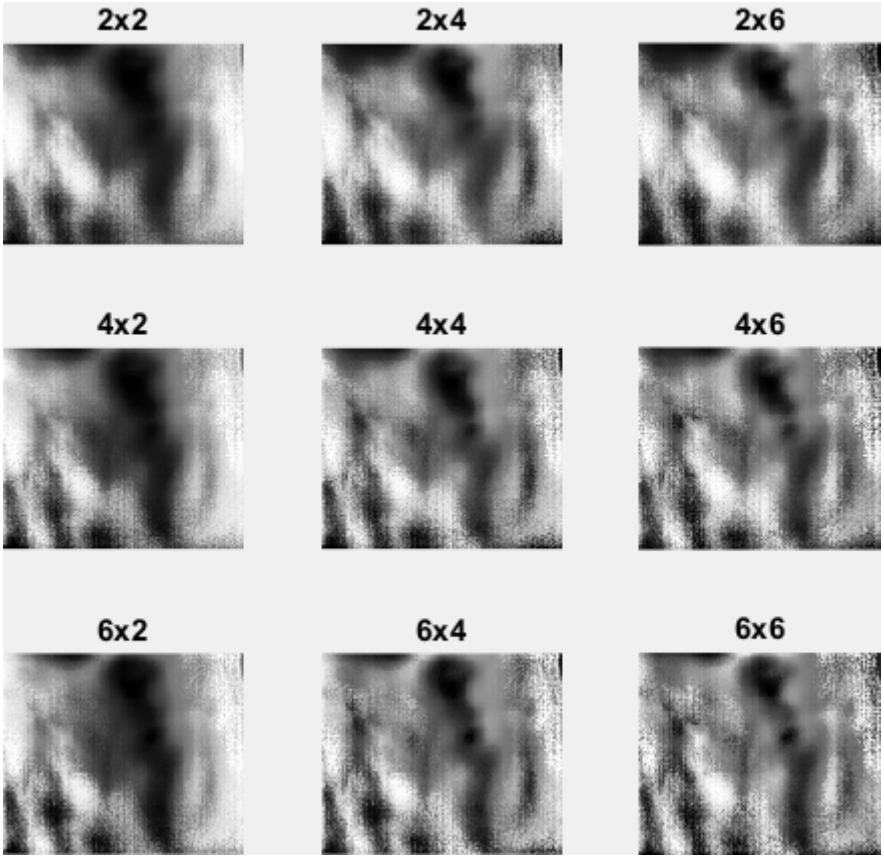

Figure 11. Variation of the size of the window for the CLAHE algorithm, and the impact on the contrast enhancement of the infrared image.

The clipping limit was also evaluated in order to define the best contrast of the image, as presented by Fig. 12. Clipping values of 3, 5, 8, 10, 13, 15, 18 and 20, as well as no clipping, were tested. It can be show from this figure that the clipping values used for this image did not limit the noise, since the image does not have a homogeneous background or any region that could justify the limitation of bins for some specific gray level. It is important to emphasize that each image has its particular parameters, and each volunteer should have their contrast analyzed.

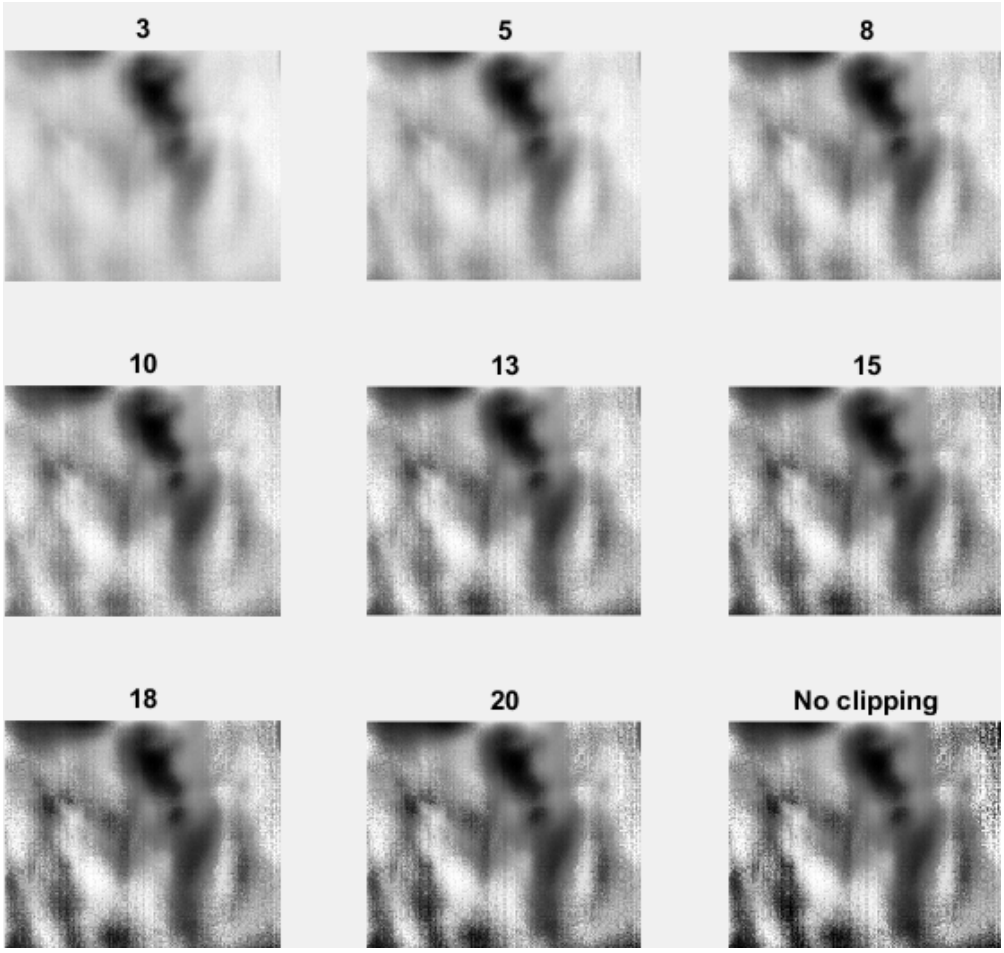

Figure 12. Variation of the clipping limit for the CLAHE algorithm, and the impact on the contrast enhancement of the infrared image.

Figure 13.a-c shows the resulting CLAHE performed for the infrared image for volunteers P1, P2 and P3, respectively, for the region described in Fig. 9.a-c. These figures show that the contrast between the thyroid gland and its surrounding organs could be greatly enhanced (see also Fig. 7.a-c) when using the local technique CLAHE, instead of the equalization of the entire image that what is presented by Fig. 10.a-c.

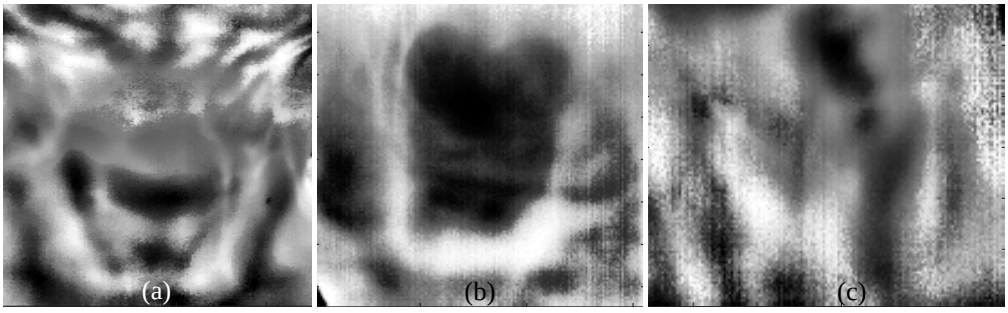

Figure 13. CLAHE in the thermographic images for the volunteer (a) P1, (b) P2 and (c) P3.

4. CONCLUSIONS

The present work aimed at the presentation of the preliminary results obtained with image processing techniques for the detection of the thyroid gland. Infrared images were obtained with three volunteers, by following a protocol that was developed in this work. The measurement protocol is important to avoid any external factors that affect the temperature measurements. The position and shape of the volunteers´ thyroid were precisely determined with ultrasound exams. The global and the local histogram equalization techniques were applied to the thermographic image. Although an increase in the image contrast could be observed with the histogram equalization, the use of the contrast limited adaptative histogram

equalization provided images with enhanced contrast that could be used for the identification of the thyroid. Such was the case because local details were lost with the global enhancement, but not with the contrast limited adaptative histogram equalization. The infrared images with the contrast limited adaptative histogram equalization image processing resulted in an accurate detection of the thyroid for the three volunteers studied in this work, which was validated with the ultrasound exams.

Future works will deal with the segmentation of the image using clustering algorithms, aiming at the autonomous detection of the thyroid gland with infrared images enhanced with image processing techniques.

5. REFERENCES

Acharya, T. and Ray, A. K., 2005. *Image Processing*. John Wiley & Sons, New Jersey, 2nd edition.

Agyingi, E., Wiandt, T. and Maggelakis, S., 2015. "Thermal detection of a prevascular tumor embedded in breast tissue". *Mathematical Biosciences and Engineering*, Vol. 12, N. 5, p. 907.

Amri, A., Pulko, S. H. and Wilkinson, A. J., 2016. "Potentialities of steady-state and transientthermography in breast tumour depth detection: A numerical study". *Computer Methods and Programs in Biomedicine*, Vol. 123, p. 68.

Carlak, H. F., Gencer, N. G. and Besikci, C., 2016. "Theoretical assessment of electro-thermal imaging: A new technique for medical diagnosis", *Infrared Physics & Technology*, Vol. 76, p. 227.

Gavriloaia, G., Ghemigian, A. M. and Gavriloaia, M. R., 2009. "Infrared Signature Analysis of the Thyroid Tumors". *Novel Optical Instrumentation for Biomedical Applications IV*, Vol. 7371, p. 73711.

Gonzalez, R. R., Woods, R. E., 1992. *Digital Image Processing*. Prentice Hall, New Jersey, 2nd edition.

Han, F., Shi, G. and Liang C., 2015. "A Simple and Efficient Method for Breast Cancer Diagnosis Based on Infrared Thermal Imaging". *Cell Biochem Biophys*, Vol. 71, p. 491.

Hummel, R., 1977. "Image Enhancement by Histogram Transformation". *Computer Graphics and Image Processing*, Vol. 6, p. 184.

Jin, C., He, Z. Z., Yang, Y. and Liu J., 2014. "MRI-based three-dimensional thermal physiological characterization of thyroid gland of human body". *Medical Engineering & Physics*, Vol. 36, p.16.

Kandlikar, S. G., Perez-Raya, I., Raghupathi, P. A., Gonzalez-Hernandez J. L., Dabydeen, D., Medeiros, L. and Phatak, P., 2017. "Infrared imaging technology for breast cancer detection – Current status, protocols and new directions". *International Journal of Heat and Mass Transfer*, Vol. 108, p.2303.

MathWorks., 2018. "Image Processing Toolbox©: User's Guide (R2018a)". Retrieved July 20, 2018 from https://www.mathworks.com/help/images/ref/histeq.html

Russ, J. J., 2002. *Image Processing Handbook.* CRC Press, Boca Ratton, 4th edition.

Santa Cruz, G.A., Bertotti, J., Marin, J., Gonzalez, S.J., Gossio, S., Alvarez, D., Roth, B.M.C., Menendez, P., Pereira, M.D., Albero, M., Cubau, L., Orellano, P. and Liberman, S.J., 2009. "Dynamic infrared imaging of cutaneous melanoma and normal skin in patients treated with BNCT". *Applied Radiation and Isotopes*, Vol. 67, p. 54.

Wahab, A. A., Salim, M. I. M., Ahamat, M. A., Manaf, N. A., Yunus, J. and Lai K. W., 2015. "Thermal distribution analysis of three-dimensional tumor-embedded breast models with different breast density compositions". *Med Biol Eng Comput*, Vol. 54, p.1363.

Zuiderveld, K., 1994. "Contrast Limited Adaptative Histogram Equalization". In Heckbert, P. S. (Ed.), *Graphics Gems IV* (474-485). Academic Press, San Diego.

.